

Bonding and magnetism in Fe- M ($M=B,C,Si,N$) alloys

A. Collins, R. C. O'Handley, and K. H. Johnson

Department of Materials Science and Engineering, Massachusetts Institute of Technology, Cambridge, Massachusetts 02139

(Received 4 September 1987)

Self-consistent-field, $X\alpha$, scattered-wave, molecular-orbital calculations on tetrahedral Fe clusters with (Fe_4-M) and without (Fe_4) central M species ($M=B,C,Si,N$) are described. The results are consistent with similar earlier calculations and go beyond those works in terms of their chemical-physical insights for bonding and magnetism. Two distinct bonding types, polar and covalent, having different consequences are identified. Polar bonding appears to play a greater role in overall stability than does covalent bonding. It mixes s and d character from Fe with s character from the M species forming new s - p - d hybrids localized largely at the M site. Its magnetic effects depend on the amount of d character lost to this bonding. On the other hand, a more covalent bonding strongly mixes Fe d character with M p character. This covalent p - d bond is delocalized relative to the initial states and can dramatically reduce the electronic state density at the Fermi level, thus suppressing moment formation.

I. INTRODUCTION

Ferromagnetism depends on the formation of local magnetic moments and on the long-range coupling of these moments. The Stoner criterion, $I(E_F)D(E_F) > 1$, gives the conditions for local-moment formation in terms of an intra-atomic exchange integral I and the paramagnetic density of states D at the Fermi level E_F . According to this criterion, $D(E_F)$ and $I(E_F)$ have to be large for the occurrence of ferromagnetism. It has been demonstrated by Yang *et al.*¹ that $I(E_F)$ is large if the wave functions at E_F are relatively localized in some region in space. This is the case for antibonding orbitals rather than bonding orbitals. The coupling interaction between the moments is described by Heisenberg's Hamiltonian $H = -\sum_{i,j} J_{ij} \mathbf{S}_i \cdot \mathbf{S}_j$ in terms of local spins \mathbf{S}_i and an interatomic exchange parameter J_{ij} . Exploitation of this long-range interaction is beyond the scope of this work.

For transition metals, moment formation and coupling are due to the interactions of the outer d electrons within atoms and between neighboring atoms, respectively. When transition metals (T) are alloyed with metalloid (M) atoms, chemical bonding takes place which changes the d - d interactions and is seen to affect the magnetic properties. There is a need for better understanding of the nature of the chemical interaction in T - M alloy and its consequences on the magnetic properties. It is the aim of this paper to explore in simple systems the details of the relation between the magnetic properties and the chemical bonding between constituents in an alloy.

In this paper we report on calculations of the electronic structure of Fe_4-M clusters based on the self-consistent-field (SCF), $X\alpha$, scattered-wave (SW), molecular-orbital (MO) (SCF- $X\alpha$ -SW-MO) method.¹ (In order to avoid confusion with specific compounds such as Fe_2B or Fe_3Si , the clusters are designated with a hyphen: Fe_4-M). This SCF- $X\alpha$ approach has been applied previ-

ously to calculate the local electronic structure of metals, alloys, semiconductors, and amorphous materials. Such calculations describe well the electronic density of states,¹ defects in semiconductors,² impurities in metals,³ chemisorption,⁴ and magnetism.¹ Metal-metalloid-cluster calculations, including Fe_4-B and Fe_4-P , were published by Messmer⁵ and details of the bonding interaction between the Fe atoms and the metalloids boron and phosphorous were elucidated. We have extended Messmer's study to include C, N, and Si in order to be able to do a comparative study of the chemical bonding and its effect on the magnetic properties. Furthermore, we are able to distinguish in our calculations polar and covalent bonding, which affect stability and magnetic properties in different ways. One of the principal advantages of this molecular-orbital method and the key to interpreting the results is the real-space topology of the calculated wave functions. Calculated orbitals, eigenvalues, and magnetic moments are considered and compared with experimental results to elucidate the effects of the chemical interaction on magnetism.

As in the case of Messmer's study, we chose the smallest Bernal polyhedron, the tetrahedron, to represent the local environment. The reasonable values calculated for the magnetic moments of such small clusters¹ and the very local nature of the important interactions in metals suggest that a tetrahedral cluster is a reasonable first approach to the problem of electronic structure of alloys. The corners of the tetrahedron are occupied by the Fe atoms and the metalloid is placed in the center. The Fe-Fe distance for the pure Fe_4 cluster was chosen to be 2.49 Å and for the Fe_4-M cluster the Fe-Fe distance was expanded to be 3.48 Å, so that a reasonable Fe-metalloid distance (2.13 Å) was obtained. This metal-metalloid distance is consistent with known distances in crystalline Fe_3P and Fe_3B ,⁶ but may not be appropriate for Fe_4-N . We do not expect each of these clusters to be the best small-cluster representation of its respective alloys. We

do expect and find useful physical insights from this simple isostructural series.

II. RESULTS

A. Energy eigenvalues

Figure 1 shows the spin-restricted (paramagnetic) molecular-orbital energy eigenvalues of the $\text{Fe}_4\text{-}M$ and the pure Fe_4 clusters. Local-density-functional (in this case, $X\alpha$) eigenvalues are Mulliken orbital electronegativities.⁷ States are labeled according to the irreducible representations of the tetrahedral group. The calculations give the relative makeup of each molecular orbital in terms of atomic s , p , or d character. The solid lines in Fig. 1 indicate occupied states and the dashed lines indicate empty states. Partial occupancy of states at E_F (which is indicated by an arrow for each cluster) is given by numbers in parentheses. The cluster density of states (DOS) obtained by Gaussian broadening of cluster eigenvalues are drawn in lighter lines over the discrete states for comparison. The positions of the free-atom levels are shown in the left-hand column. The eigenvalue spectra of all five clusters consist of a narrow d band delimited by the $1t_2$ and $2t_1$ levels, overlapped by levels of higher s - p character ($1a_1, 2a_1, 3a_1, 4t_2, 3e$), which are representative of the wide s - p band found in bulk iron. Table I summarizes some important features of the eigenvalue spectra and compares them to the Fe_4 values. The net spin per Fe atom is determined by running the program in the spin-unrestricted mode. $E_F - E(1a_1)$ and $E_F - E(1t_2)$ indicate the positions of the bottoms of the conduction and d bands, respectively. The energy range $E(2t_1) - E(1t_2)$ contains states of predominantly d char-

acter and thus gives a relative measure of d -band width. The last row of the table gives the exchange splitting averaged over the states within the d band as defined above. We observe a dramatic lowering of the bottom of the conduction band and an increase of the width of the d band upon metalloid addition. The average d - d exchange splitting is reduced for all metalloid-containing clusters, and the net spin per atom is strongly suppressed for $\text{Fe}_4\text{-C}$ and $\text{Fe}_4\text{-N}$.

B. Molecular orbitals

Before we can discuss the implications for bonding and magnetism of these cluster orbital eigenvalues we must consider their orbital character and spatial localization. In Figs. 2 and 3 the $1a_1$ and $1t_2$ orbitals are shown, respectively. These orbitals are plotted in the (110) plane, which includes two iron atoms in the upper corners of the plane and the metalloid atom in the center. The solid lines indicate wave functions of positive phase and the dashed lines indicate negative phase. Bonding orbitals are identified by merging of orbitals of the same phase between two atoms. See, for example the $1a_1$ orbital of Fe_4 (Fig. 2). Antibonding orbitals are characterized by a nodal plane between two atoms. An example of this is seen in the $1t_1$ orbital of Fe_4 (Fig. 4). Below each MO, the distribution (in percent) of the orbital between the Fe and M sites is indicated. The breakdown of this orbital at each site into s , p , and d character is also shown. Finally, the delocalization of the orbital outside the atomic spheres but within the sphere around the entire cluster or outside of the cluster sphere is indicated. A buildup of charge between atoms is indicative of delocalization that accompanies covalent bonding.

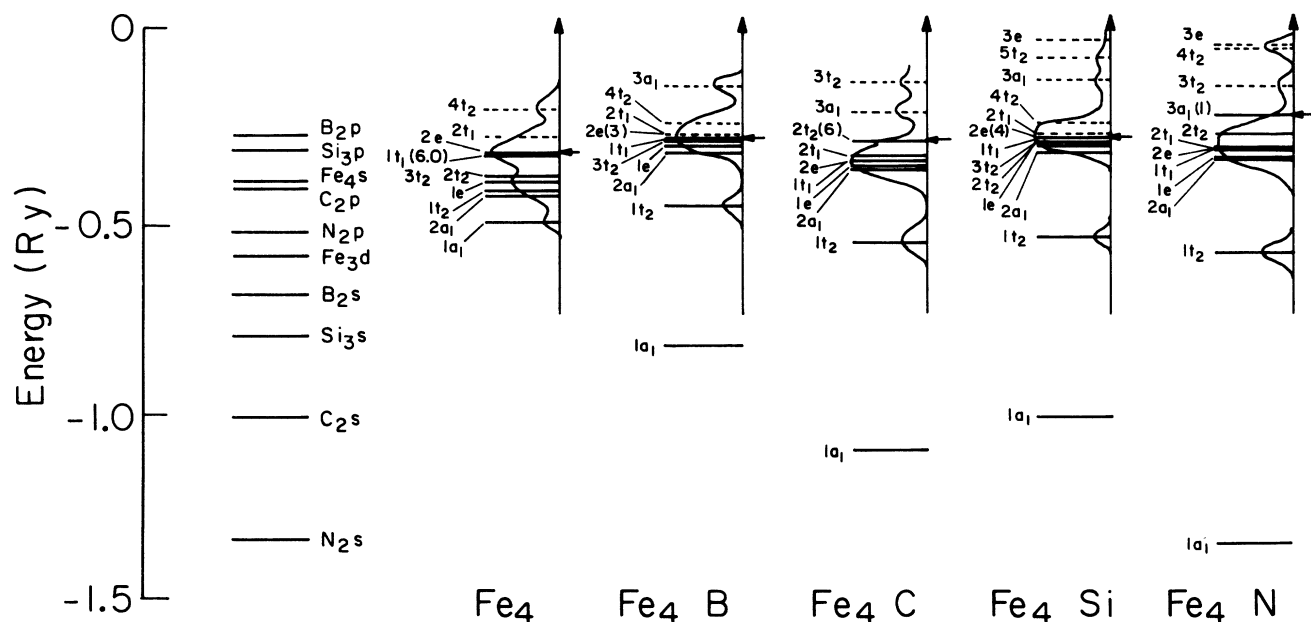


FIG. 1. Molecular-orbital energy levels and density of states for Fe_4 and $\text{Fe}_4\text{-}M$ clusters ($M=\text{B, C, N, Si}$). Free-atom eigenvalues are shown at the left for comparison.

TABLE I. Comparison of spin-unrestricted Fe₄-M (M=B,N,Si) cluster results with those of Fe₄ cluster. For Fe₄-C we used spin-restricted results because the spin-unrestricted calculation indicated zero magnetic moment (energies in eV).

	Fe ₄	Fe ₄ -B	Fe ₄ -C	Fe ₄ -Si	Fe ₄ -N
Net spin (in units of μ _B /Fe-atom)	3.0	3.25	0.0	3.0	0.26
E _F -E(1a ₁)	↑ 4.4 ↓ 3.3	8.0 7.6	10.7	10.3 10.0	15.2 15.0
E _F -E(1t ₂)	↑ 3.7 ↓ 1.4	3.5 2.5	3.4	4.5 3.6	4.9 4.7
E(2t ₁)-E(1t ₂) with of d band	↑ 1.7 ↓ 2.3	1.7 2.7	2.8	2.8 3.9	3.8 3.7
Average d-d splitting	2.6	1.8	0.0	1.7	0.2

All of the valence-band molecular orbitals involve substantial Fe *d* character and varying amounts of Fe *p* and *s* character. The Fe orbitals are mixed mostly with metalloid *s* character in the 1a₁ orbital (Fig. 2) and with metalloid *p* character in the 1t₂ orbital (Fig. 3). The tables below each orbital clearly show the reduction of Fe *d*

character on going from the *d-d*-bonded Fe₄ tetrahedron to the *sp-d*-bonded Fe₄-M cluster.

Figure 4 shows the orbital character of the states at E_F. Here we see states of t₁, t₂, and a₁ as well as *e* symmetry (for Fe₄-B and Fe₄-Si) which, because of their orientation, remain totally *d*-like, unmixed with any

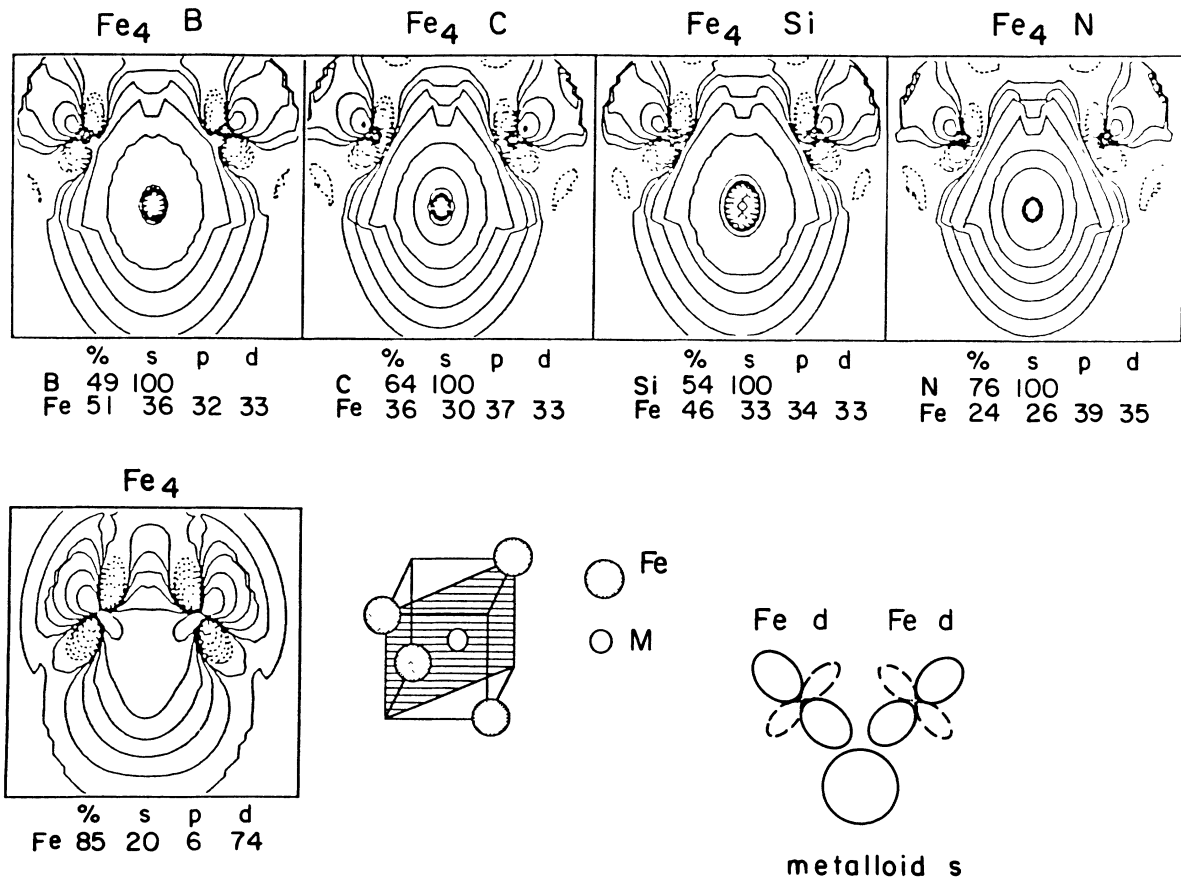


FIG. 2. 1a₁ molecular orbital for Fe₄ and Fe₄-M (M=B,C,N,Si) clusters. The cluster geometry, projection plane (110), and a schematic diagram of the metalloid *s* and the iron *d* contributions are indicated.

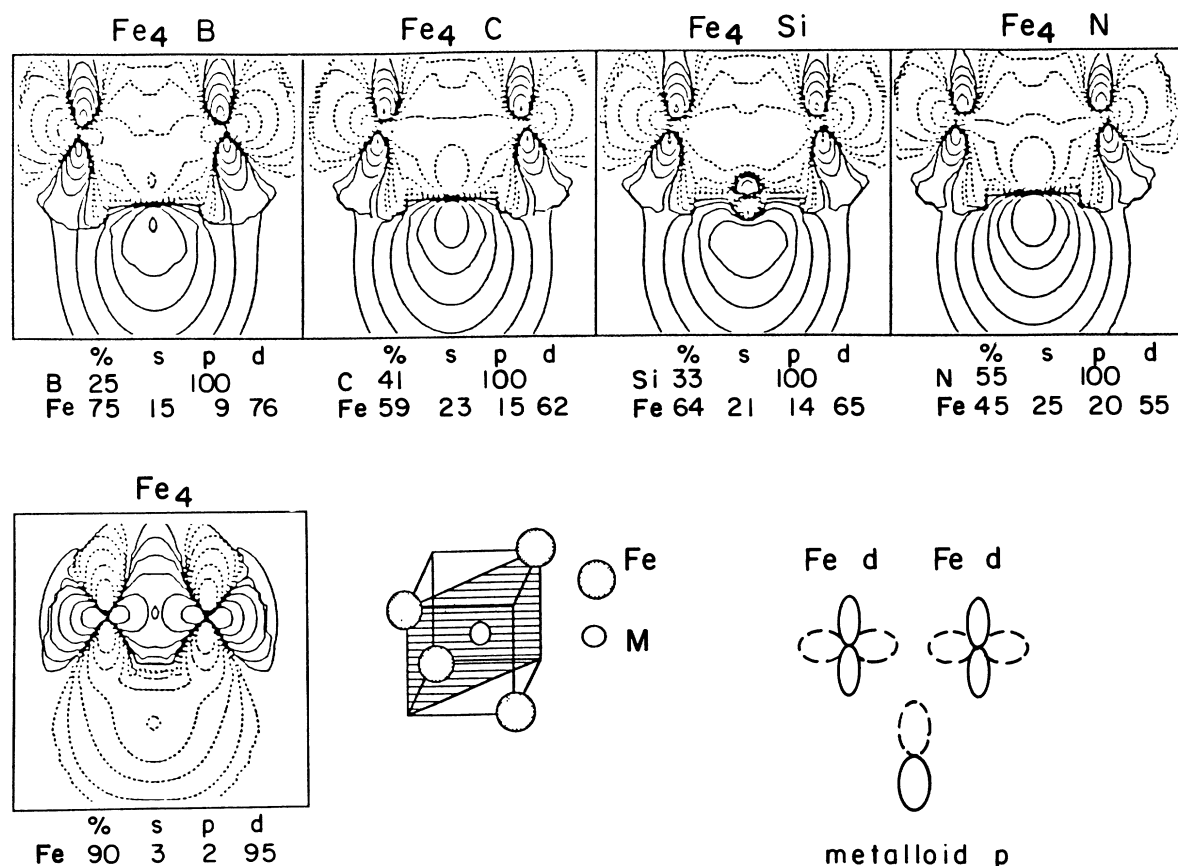


FIG. 3. $1t_2$ molecular orbital for Fe_4 and $\text{Fe}_4\text{-M}$ ($M=\text{B}, \text{C}, \text{N}, \text{Si}$) clusters. The cluster geometry projection plane, and a schematic diagram of the metalloid p and the iron d contributions are indicated.

metalloid s or p character. The behavior of the e orbitals contrasts sharply with that of the less- d -like orbitals at E_F in $\text{Fe}_4\text{-C}$ and $\text{Fe}_4\text{-N}$, which show significant p - d and s - d hybridization, respectively.

III. DISCUSSION

By far, the levels most sensitive to the presence of metalloids are the lowest ones, $1a_1$ and $1t_2$. Relative to the Fe_4 cluster we observe a strong lowering of the $1a_1$ level and a smaller lowering of the $1t_2$ level with the addition of metalloids (Fig. 1). These effects indicate that significant chemical bonding of the Fe with the metalloids takes place. The amount of the lowering of the $1a_1$ and $1t_2$ levels relative to the Fe atomic d level is a good measure of the strength of the chemical bonding. As we can see from Fig. 1, the $1a_1$ and $1t_2$ levels of $\text{Fe}_4\text{-C}$ and $\text{Fe}_4\text{-N}$ lie lower than the $1a_1$ and $1t_2$ levels of the $\text{Fe}_4\text{-B}$ and $\text{Fe}_4\text{-Si}$. Therefore we conclude that C and N should form stronger bonds with tetrahedral Fe than B and Si do.

A. Chemical bonding

The chemical-bonding interactions that affect the electronic states and determine the physical properties can be

reduced to two main types: polar bonds and covalent bonds. Polar bonds are formed between orbitals of two atoms A and C (anion and cation) that differ significantly in their electronegativities (the difference in the electronegativities is a measure of the polarity), whereas covalent bonds are formed between orbitals that have similar electronegativities (i.e., similar electronic energies $E_A = E_C$).⁸ In both cases the orbitals must satisfy symmetry and overlap conditions as well.

From the positions of the free-atom eigenvalues (orbital electronegativities⁷) in Fig. 1 it is reasonable to expect that the bonding between the Fe $3d$ level and the lower-lying metalloid s states will be largely polar in character and stronger for N and C whose s orbitals are most electronegative relative to Fe $3d$. Similarly, the four metalloid atomic p states immediately above the Fe $3d$ state will form a predominantly covalent p - d orbitals with the greatest covalent mixing taking place between Fe and N or C. We will now show how these expectations are realized in the cluster calculations.

For the pure Fe_4 cluster, the $1a_1$ orbital (Fig. 2) exhibits its mostly d character (74%). The addition of the metalloids stabilizes the $1a_1$ level by polar hybridization between the metalloids levels ($2s$ for B, C, and N, or $3s$ for Si) and the iron $3d$ levels. The charge-density contours (Fig. 2) and the tables below them reveal the polarity of

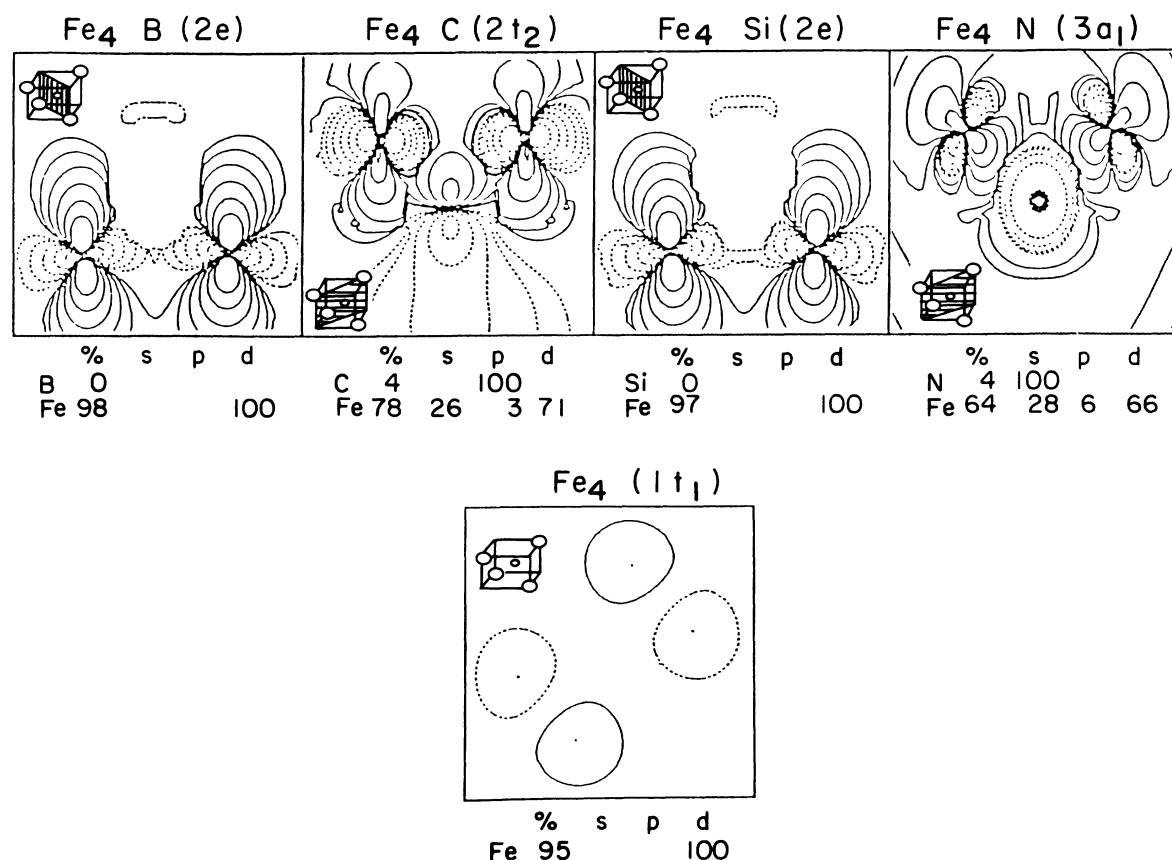


FIG. 4. Highest occupied molecular orbitals: Fe₄ (1t₁), Fe₄-B (2e), Fe₄-C (2t₂), Fe₄-Si (2e), and Fe₄-N (3a₁). The projection planes are shown. The 1t₁ orbital is projected in a parallel plane above (001).

the bond. In the formation of a polar bond, charge is transferred from the orbital of higher energy (lower electronegativity) to that of lower energy (higher electronegativity). As a result of this charge transfer, the bond is biased toward the more electronegative species, which in this case is the metalloid. Indeed, we observe in Fig. 2 for the 1a₁ orbital a high percentage of charge density concentrated on the metalloid site. The percentage of electronic charge density at the metalloid site that is involved in the *s-d* bonding is larger for C and N (64% and 76%, respectively) than for B and Si (49% and 54%, respectively) because of the greater electronegativity of C and N.

The character of the 1t₂ orbital for all the clusters is shown in Fig. 3. The pure Fe₄ 1t₂ orbital is mostly *d*-like. The addition of the metalloids causes covalent hybridization between the *p* levels of the metalloids and the Fe 3*d*. This *p-d* hybridization results in a delocalization of the *d* orbitals and a reduction of the atomic *d* character. This is clearly seen in the greater spatial extent of the *d*-like wave functions about Fe atoms in Fig. 3 compared to those in Fig. 2. Thus the increase of the *d*-band width discussed above is due to covalent bonding and indeed is found to be greater for C- and N-containing clusters. Figure 3 shows the *p-d* character of this covalent orbital, and the tables below each orbital indicate the greatest loss of *d* character of this bond for C and N.

B. Magnetism

As is well known, the origin of magnetism can be attributed to intra-atomic and interatomic *d-d* exchange interactions. Therefore as the *d* character of the wave function is diluted by *s-d* or *p-d* hybridization, the tendency toward magnetic-moment formation and long-range moment coupling is reduced. The moment reduction is indicated in the calculated spin moment per iron atom listed in Table I.

For C and especially for N, the covalent *p-d* hybridization with Fe is largely due to the small energy difference between the initial atomic states (Fig. 1). Calculated charge-density distributions corresponding to the molecular orbitals near *E_F* (Fig. 4) do indeed show large delocalization and *p-d* mixing. This results in increased interatomic charge indicative of delocalized character and leaves the Stoner product *I*(*E_F*)*D*(*E_F*) low. Thus C and N reduce the moment to 0 and 0.25 μ_B/Fe-atom, respectively, in these tetrahedral clusters.

On the other hand, B and Si atomic *p* states lie well above the atomic Fe 3*d* state and therefore they show only weak covalent hybridization. Calculated charge-distribution contours of the molecular orbitals at *E_F* (Fig. 4) show that the B and Si *p* orbitals do not contribute at all to this orbital, which has 100% *d* character. Consequently, *I*(*E_F*)*D*(*E_F*) remains high for these clusters

and the spin-unrestricted $\text{Fe}_4\text{-B}$ and $\text{Fe}_4\text{-Si}$ cluster calculations give large moments, 3.2 and 3.0 $\mu_B/\text{Fe-atom}$, respectively (Table I).

The calculated moments are reasonably consistent with experimental results if you keep in mind the small clusters studied and the tendency of the $X\alpha$ method to overestimate moment formation. Amorphous $\text{Fe}_{80}\text{B}_{20}$ shows a saturation moment of approximately 2.1 $\mu_B/\text{Fe-atom}$.⁹ Addition of C to $\text{Fe}_{80}\text{B}_{20}$ glasses suppresses the saturation moment.¹⁰ Amorphous $\text{Fe}_{80}\text{Si}_{20}$ thin films show a magnetic moment of 2.0 $\mu_B/\text{Fe-atom}$.¹¹ $\text{Fe}_{1-x}\text{N}_x$ thin films show a large moment at low N concentration with strong reduction of the Fe moment for increasing x .¹²

The idea that the moment suppression is a result of the loss of d character by the magnetic states because of hybridization with the p metalloid states, rather than because of charge transfer, was suggested by Alben, Budnick, and Cargill.¹³ Early experimental evidence for p - d hybridization was given by Allen, Wright, and Connell.¹⁴ While Messmer's $\text{Fe}_4\text{-B}$ and $\text{Fe}_4\text{-P}$ cluster results gave some insight into the transition-metal-metalloid bonding, here we clearly see the covalent nature of the p - d bonding, its strong effect on magnetic moment, and, finally, significant variation of these bonding and/or magnetic effects with metalloid type.

Charge transfer from one species to another can occur for a particular orbital involved in polar bonding. However, this will be compensated for by transfer in the oppo-

site sense for other orbitals to preserve overall charge neutrality in these metallic alloys. This was demonstrated by Watson and Bennett.¹⁵ Our cluster calculations show Fe d character from the $1a_1$ orbitals in Fe_4 transferred to M sites in $\text{Fe}_4\text{-}M$ clusters (Fig. 2). It is not possible to determine the compensating M -to-Fe charge transfer because we do not have orbitals for pure- M clusters.

IV. SUMMARY

SCF- $X\alpha$ -SW-MO calculations on clusters representative of $\text{Fe}_{80}M_{20}$ -type glasses show two types of bonding, polar s - d bonding and covalent p - d bonding. The strength of the polar s - d bonding increases with increasing electronegativity difference of the initial orbitals and is responsible for the overall stability of the alloy. On the other hand, the covalent p - d bonding increases with decreasing electronegativity difference and depends upon the amount of overlap between the Fe $3d$ band and the metalloid p band and therefore it strongly affects the magnetic properties.

ACKNOWLEDGMENTS

We gratefully acknowledge support of this work by the 3M Company. Help with the use of the $X\alpha$ programs and discussion of the results with Michele Donovan and Mike McHenry are sincerely appreciated.

¹C. Y. Yang, K. H. Johnson, D. R. Salahub, J. Kaspar, and R. P. Messmer, Phys. Rev. B **24**, 5673 (1981).

²R. P. Messmer and G. D. Watkins, Phys. Rev. B **7**, 2468 (1973).

³K. H. Johnson, D. D. Vvedensky, and R. P. Messmer, Phys. Rev. B **19**, 1519 (1971).

⁴A. J. Bennet, B. McCarroll, and R. P. Messmer, Phys. Rev. B **3**, 1397 (1971).

⁵R. P. Messmer, Phys. Rev. B **23**, 1616 (1981).

⁶S. Rundquist, Acta. Chem. Scand. **61**, 1 (1962); **61**, 242 (1962); **61**, 992 (1962).

⁷M. E. McHenry, R. C. O'Handley, and K. H. Johnson, Phys. Rev. B **35**, 3555 (1987).

⁸W. A. Harrison, *Electronic Structure and the Properties of Solids* (Freeman, San Francisco, 1980).

⁹R. C. O'Handley, R. Hasegawa, R. Ray, and C. P. Chu, Appl. Phys. Lett. **29**, 330 (1976).

¹⁰K. S. Kazama, M. Mitera, and T. Masmumoto, in *Proceedings of the Third International Conference on Rapidly Quenched Metals*, edited by B. Cantor (The Metals Society, London, 1978), Vol. II, p. 164.

¹¹G. Marchal, P. Magnin, M. Piecuch, C. Janot, and J. Hubsch, J. Phys. F **7**, 165 (1977).

¹²M. Nagakubo and M. Naoe (unpublished).

¹³R. A. Alben, J. I. Budnick, and G. S. Cargill, in *Metallic Glasses*, edited by J. J. Gilman and H. J. Leamy (American Society of Metals, Metals Park, Ohio, 1978).

¹⁴J. W. Allen, A. C. Wright, and G. A. N. Connell, J. Non-Cryst. Solids **40**, 509 (1980).

¹⁵R. E. Watson and L. H. Bennett, in *Theory of Alloy Phase Formation*, edited by L. H. Bennett (The Metallurgical Society of AIME, New York, 1980), p. 425.

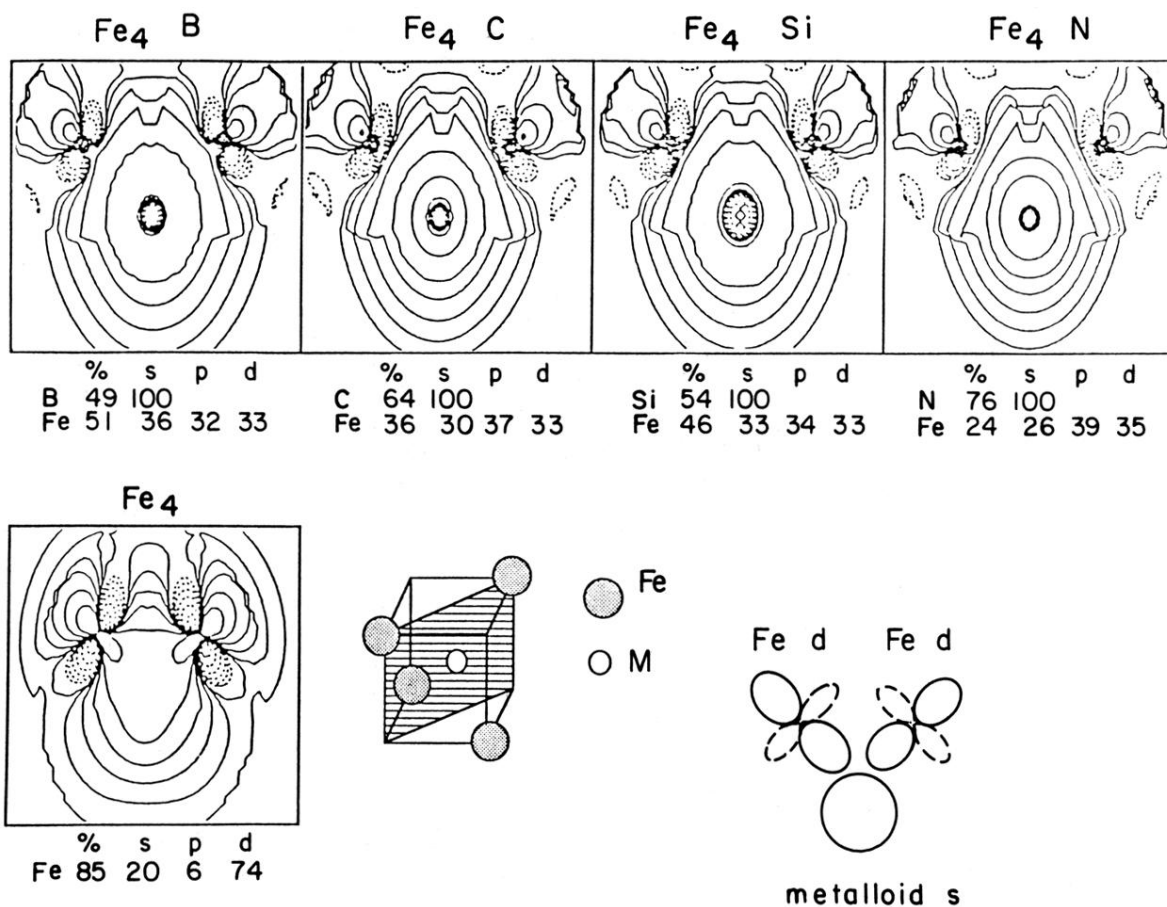


FIG. 2. $1a_1$ molecular orbital for Fe_4 and $\text{Fe}_4\text{-M}$ ($M=\text{B}, \text{C}, \text{N}, \text{Si}$) clusters. The cluster geometry, projection plane (110), and a schematic diagram of the metalloid s and the iron d contributions are indicated.

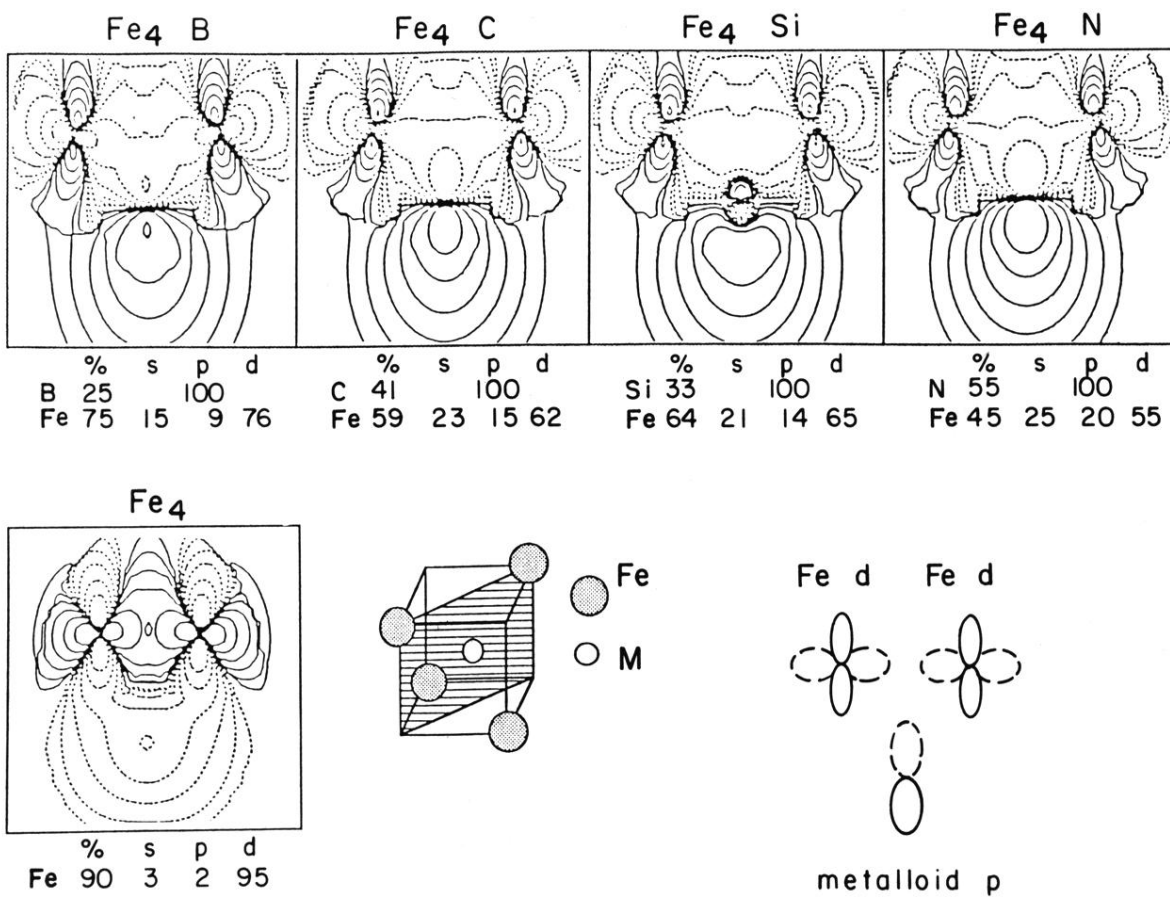


FIG. 3. $1t_2$ molecular orbital for Fe_4 and $\text{Fe}_4\text{-M}$ ($M=\text{B}, \text{C}, \text{N}, \text{Si}$) clusters. The cluster geometry projection plane, and a schematic diagram of the metalloid p and the iron d contributions are indicated.